Second-order ionospheric term in GPS: Implementation and impact on geodetic estimates

M. Hernández-Pajares,[1] J. M. Juan,[1] J. Sanz,[1] and R. Orús[1,2]

Received 22 August 2006; revised 22 May 2007; accepted 5 June 2007; published 29 August 2007.

[1] In this paper, different aspects of the application of the second-order ionospheric term (abbreviated as I_2) and its impact on geodetic estimates are studied. A method to correct the GPS observations from this effect is proposed. This method provides a more accurate correction to the GPS measurements (in some cases, it can even be 50% better) with respect to other ways of computing such effect. Moreover, this method can be applied routinely to estimate geodetic parameters. Applying the I_2 correction to subdaily differential positioning, several relationships between the deviation of the parameter estimates and the I_2 term are derived in the context of a new global approach to the problem. In particular, it is shown that the effect in receiver position mainly depends on the differential value of this term between GPS receivers, while the satellite clocks are directly affected by the undifferenced values. Data from the International GNSS Service (IGS) global network of receivers have been gathered over a period of 21 months. These data have been used to study the I_2 effect on the geodetic estimates, such as receiver positions, satellite clocks, and orbits. The most important effect appears for the satellite clocks, and it can be greater than 1 cm depending on the geographical location, comparable to the IGS nominal accuracies. The effect on orbits consists of a global contribution of several millimeters (which confirms the geocenter displacement detected by other authors) plus a subdaily contribution, also of several millimeters, that is geographically dependent, also comparable to the IGS nominal accuracies. As for the position of receivers, the obtained shifts are, in general, at submillimeter level and are directed southward for low-latitude receivers and northward for high-latitude receivers. These results will be explained in detail since they are not completely in agreement with the ones presented in previous works.

Citation: Hernández-Pajares, M., J. M. Juan, J. Sanz, and R. Orús (2007), Second-order ionospheric term in GPS: Implementation and impact on geodetic estimates, *J. Geophys. Res.*, *112*, B08417, doi:10.1029/2006JB004707.

1. Introduction

[2] As is well known, Global Positioning System (GPS) observations are affected by the ionospheric refraction (see, e.g., *Klobuchar* [1978] or *Lanyi and Roth* [1988]). The main contribution of this ionospheric refraction (99.9%) corresponds to the first order ionospheric term, which is inversely proportional to the square of the frequency. Therefore this term can be removed from the GPS observations when considering the carrier phase or the code ionospheric free combinations (L_c and P_c, respectively). However, because of the increasing demand for improvements in precise GPS positioning, the study of the impact of the second-order ionospheric term (I_2) has become relevant. I_2 is proportional to the magnetic field (**B**) projection along the transmitter-receiver direction ($B\cos\theta$) and the ionospheric delay of the signal, which is related to the slant total electron content (STEC), being defined as follows (in electrons/m^2 units):

$$\mathrm{STEC} = \int_{\mathrm{rec}}^{\mathrm{sat}} N_e ds \tag{1}$$

where N_e stands for the ionospheric electron density (in electrons/m^3) and ds represents, in meters, the differential length of GPS line of sight (LOS) ray.

[3] In this context, the impact of I_2 on accurate positioning was already studied by *Kedar et al.* [2003] under high-ionization conditions: Solar maximum scenario (2000–2002) monitoring low-latitude GPS receivers. The I_2 corrections were computed using a dipolar model of the geomagnetic field, the Jet Propulsion Laboratory Global Ionospheric Mapping Software [see *Mannucci et al.*, 1998] as well as a precise point positioning (PPP) approach, assuming that satellite clocks and orbits were not affected by the second-order ionospheric term (i.e., the I_2 corrections

[1] Research Group of Astronomy and Geomatics, Technical University of Catalonia, Barcelona, Spain.
[2] Now at Wave Interaction and Propagation Section, European Space Research and Technology Centre, European Space Agency, Noordwijk, Netherlands.

0148-0227/07/2006JB004707$09.00

were only adjusted to the receiver parameters). One of their main conclusions was that a global southward displacement of several millimeters was detected in the positions of the receivers, when following their strategy.

[4] In a later study by *Fritsche et al.* [2005] and *Steigenberger et al.* [2006] went one step further considering the adjustment of additional parameters such as satellite orbits and Earth rotation parameters. In this way they overcome the limitations of the PPP positioning strategy used by *Kedar et al.* [2003] as we do in this work. Their results confirmed as well the southward displacement in the receiver position, but its magnitude reduced around 50%, in such a way that it only remained remarkable in the Southern Hemisphere. *Fritsche et al.* [2005] also showed how I_2 affected the geocenter estimation, obtaining a significant displacement of several millimeters along the Z axis when considering I_2, being this displacement correlated with the ionospheric cycles.

[5] Besides improving the understanding of the I_2 effect on receiver positions, the goal of this work is to show how it also affects other parameters, such as satellite clocks and orbits, providing their relationship with I_2 values, and complementing and clarifying the conclusions obtained by previous authors. To perform such tasks, several positioning strategies are used and will be explained in sections 2–4.

[6] In section 2, the developed strategy to obtain and apply the I_2 correction is presented. This explanation is needed because the strategy is different from the ones used by *Kedar et al.* [2003] and *Fritsche et al.* [2005], emphasizing the advantages in terms of accuracy and simplicity. In section 3, the I_2 effect on subdaily differential positioning is shown when considering a simple model, showing that at such scale, the effect can be significantly important. Finally, in section 4, the I_2 effect on geodetic estimates is studied applying a complete global model that computes receiver positions, satellite orbits and clocks, among other terms.

2. Computing and Applying the I_2 Correction

[7] When the I_2 effect is considered, the expressions for both ionospheric-free carrier phases and pseudoranges (L_c and P_c) can be expressed as follows [see *Bassiri and Hajj*, 1993]:

$$L_c = \frac{f_1^2 L_1 - f_2^2 L_2}{f_1^2 - f_2^2} = \rho + \frac{s}{2 f_1 f_2 (f_1 + f_2)} + b_c \tag{2}$$

$$P_c = \frac{f_1^2 P_1 - f_2^2 P_2}{f_1^2 - f_2^2} = \rho - \frac{s}{f_1 f_2 (f_1 + f_2)} \tag{3}$$

where L_i and P_i are the carrier phase and code measurements (in meters) at frequency f_i, being f_1 = 1.57542 GHz and f_2 = 1.22760 GHz; ρ is the geometrical distance plus other nondispersive terms; and b_c is the L_c carrier phase ambiguity. The I_2 effect on L_c and P_c is driven by the s term, which is defined, in System International units (SI or MKS units), as

$$s = 7527 c \int_{\text{rec}}^{\text{sat}} N_e B \cos\theta \, ds \tag{4}$$

where c stands for the speed of light, N_e is the free-electron density, B is the module of the Earth's magnetic field (**B**), and θ is the angle between **B** and the propagation direction, being the integral performed over the LOS.

[8] If it is assumed that the ionosphere is modeled as a single layer at a certain altitude (450 km, in this work), **B** will correspond to the magnetic field at the ionospheric pierce point (IPP) and equation (4) can be rewritten as

$$s = 7527 c B \cos\theta \, \text{STEC} \tag{5}$$

The second term in the right member of equations (2) and (3) corresponds to the I_2 term effect on L_c and P_c. It is noticeable that the I_2 term is identical between L_c and P_c except for the sign and a factor of 2. In case I_2 was neglected, this will introduce some mismodeling in the carrier phase ambiguity estimation, as shown in detail in section 3.

[9] From now on, I_2 will be considered as the correction that has to be applied to L_c in order to correct it from such effect. Taking into account this definition and equation (2), I_2 can be written as

$$I_2 = -\frac{s}{2 f_1 f_2 (f_1 + f_2)} \tag{6}$$

In this way and according to (5), the I_2 correction depends on both STEC and the module of the magnetic field **B**. *Kedar et al.* [2003] and *Fritsche et al.* [2005] computed STEC using global ionospheric maps (GIM) or a dedicated GIM software. In fact, this GIM provides the vertical total electron content (VTEC) that has to be converted into STEC applying a mapping function. In this work, an alternative way to compute STEC is followed, based on the GPS geometry-free combinations in phase and code (L_I and P_I). For each receiver-transmitter pair, such combinations can be written, in first-order approximation, as

$$L_I = L_1 - L_2 = \text{STEC} + b_I + K_{\text{sat}} + K_{\text{sta}} \tag{7}$$

$$P_I = P_2 - P_1 = \text{STEC} + K_{\text{sat}} + K_{\text{sta}} \tag{8}$$

where b_I is the carrier phase ambiguity corresponding to L_I, K_{sat} is a satellite-dependent instrumental delay and K_{sta} is a station-dependent instrumental delay (all of them expressed in meters).

[10] As L_I is much more precise than P_I, STEC will be obtained from (7). Nevertheless, the bias term b_I will have to be calculated by applying an alignment between L_I and P_I.

$$\text{STEC} = L_I - \langle L_I - P_I \rangle - K_{\text{sat}} - K_{\text{sta}} \tag{9}$$

where the angle brackets denote the mean value within the same continuous carrier phase arc of data corresponding to a transmitter-receiver pair. The main advantage of computing STEC using equation (9), is that the I_2 computation is easier since K_{sta} and K_{sat} are quite constant over time, and can be calculated considering their previous values and not requiring a previous or a simultaneous GIM computation. Therefore it can be easily implemented in geodetic computations.

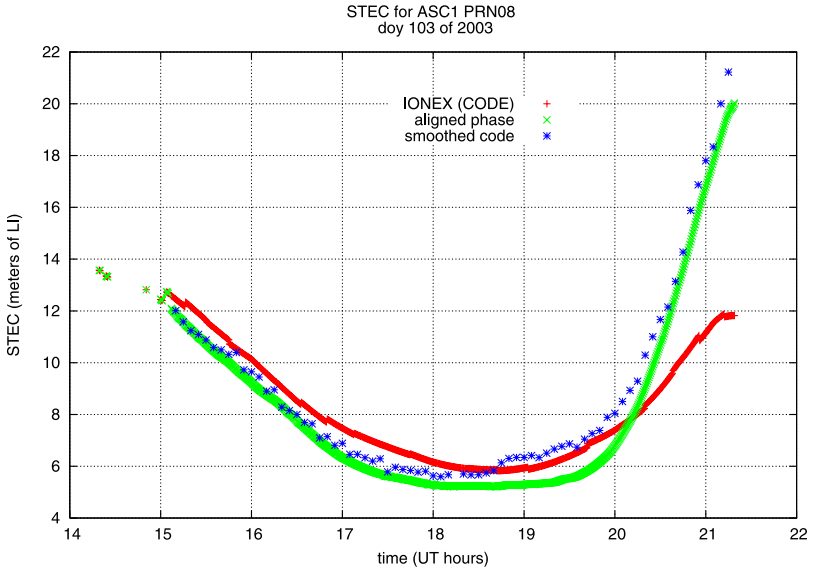

Figure 1. STEC comparison estimated using a GIM (CODE IONEX file, red line) and using the method of code alignment proposed in this work (taking the instrumental delays from the same IONEX file, blue points). Both estimations are compared with the ground truth provided by the geometric-free combination of carrier phases (L_I), in green. The data correspond to the ASC1 receiver (14W08S), day 103 of 2003.

[11] As K_{sta} and K_{sat} instrumental delays are estimated with an error generally better than 1 ns [see *Hernández-Pajares*, 2004], such errors can be neglected. In fact, their contribution to I_2 would be at the submillimeter level on range, the same error level than using GIMs for the computations (as in the previous works). Actually, for low-latitude receivers, STEC predictions are usually better in this approach than using GIMs. This is due to the lack of receivers at such latitudes because the computation of GIMs is mainly driven by interpolation (required to fill the gaps in the data spatial distribution), coinciding with a high STEC variability. In Figure 1, those two ways of computing STEC are compared for PRN08 tracked by the IGS receiver ASC1 (14W08S). As it can be seen, STEC computed using a GIM

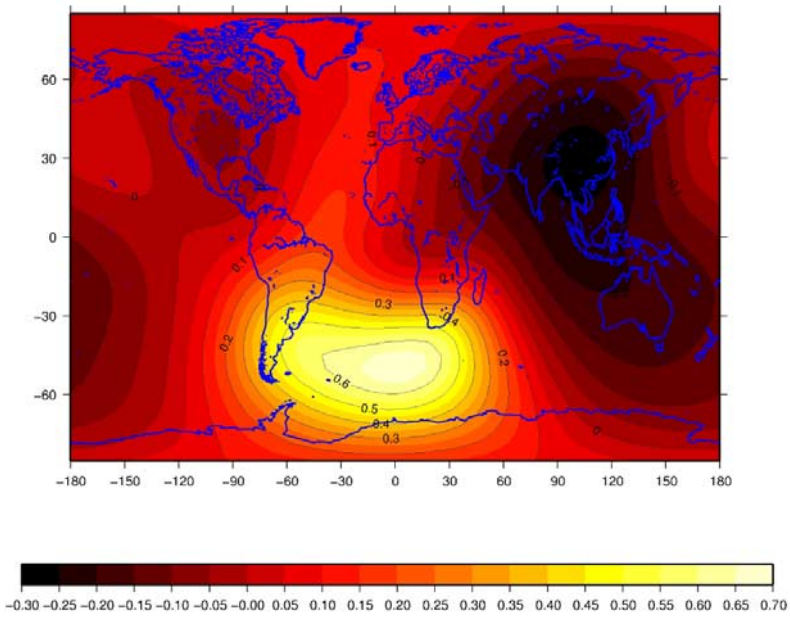

Figure 2. Relative difference between the magnetic field intensity provided by the dipolar model and the more realistic International Geomagnetic Reference model, referred to this last one (DOY 69 of year 2001).

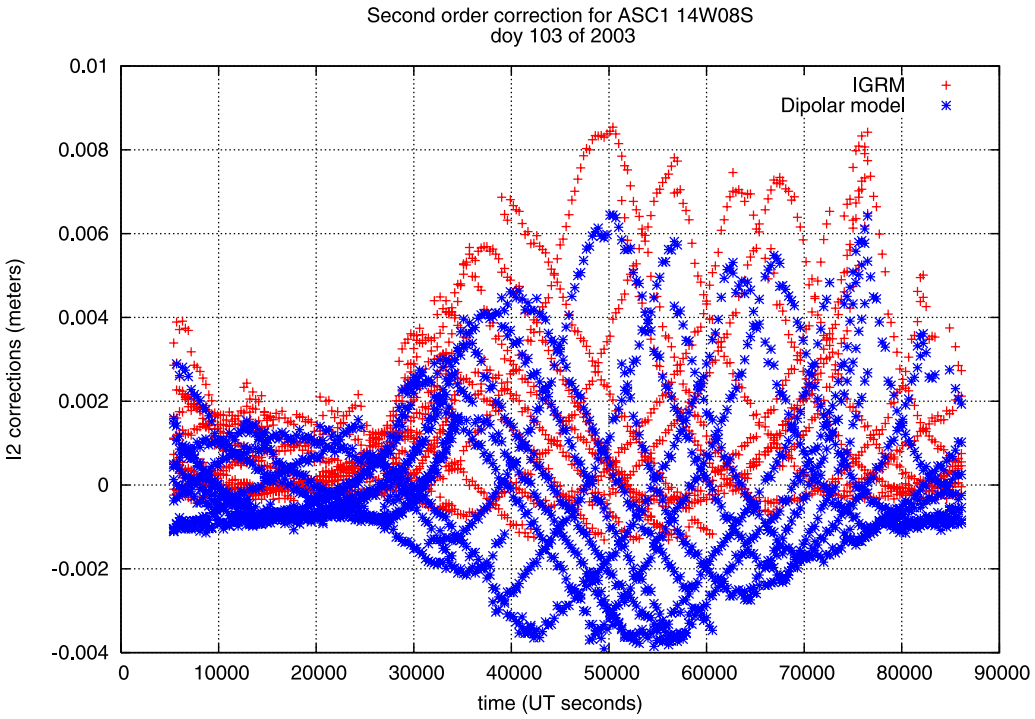

Figure 3. I_2 correction for the IGS receiver ASC1 (14W08S), computed using the IGR model (crosses) and the dipolar model (asterisks). The data correspond to DOY 103 of year 2003.

can introduce errors up to 50%, at low latitudes and low elevations, when the I_2 effect becomes more relevant (specially in solar maximum conditions).

[12] Another difference with respect to previous works when computing I_2 is regarding the geomagnetic field dependence: instead of a simple dipolar model, a more realistic model is used, the International Geomagnetic Reference Model (IGRM), provided by Geopack subroutines [*Tsyganenko*, 2003].

[13] As depicted in Figure 2, the relative difference between both geomagnetic field models ranges from −20% in the east of Asia up to +60% in the so-called South Atlantic Anomaly (SAA). This difference directly affects the I_2 corrections. This can be appreciated in Figure 3 where the computation of I_2 is plotted using both models for the receiver ASC1. These comparisons strongly suggest the convenience of using a more realistic magnetic model, such as IGRM or others of public availability (see, for instance, http://www.ngdc.noaa.gov/seg/geomag/models.shtml).

3. Effect on Subdaily Differential Positioning

[14] Before facing the study of the I_2 correction impact on the global estimation of geodetic parameters, its effect on a simpler scenario, subdaily differential positioning, is going to be analyzed. There are two main reasons that justify this study:

[15] 1. The subdaily relative variations of the I_2 corrections are larger than for longer periods (such as daily or

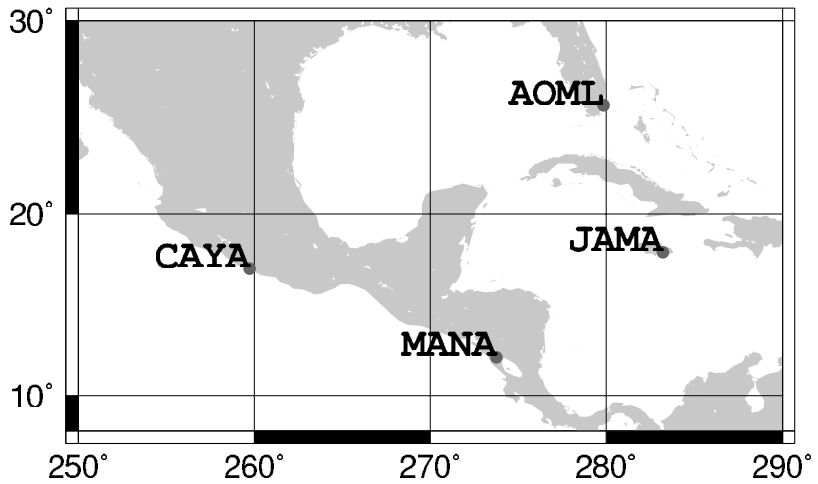

Figure 4. Location of the IGS receivers used in the subdaily strategy study.

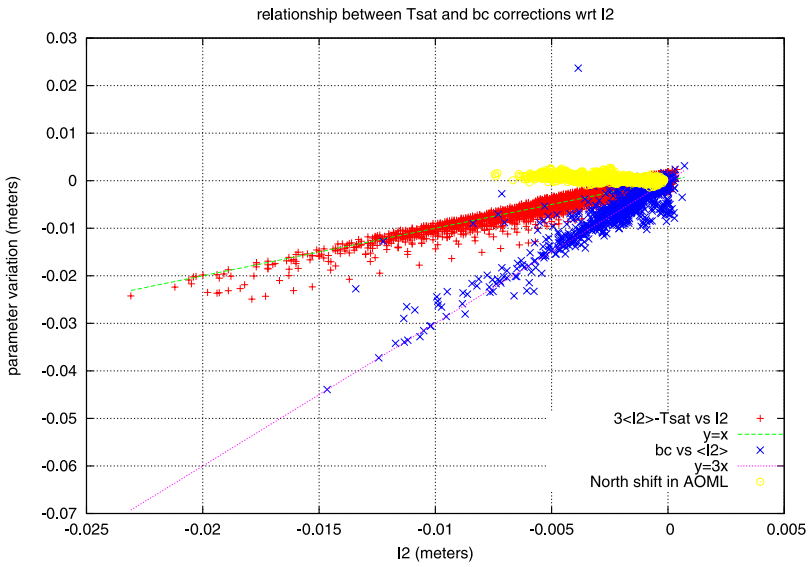

Figure 5. Effect of the I_2 correction on several parameter estimations, using a differential strategy, confirming the relationships (12), blue points, and (13), red points. The data correspond to receiver JAMA (DOYs 065–071 of year 2001).

seasonal periods) so bigger displacements of the coordinates should be expected.

[16] 2. The differential positioning model is generally simpler than a global model, allowing to better understand the relationships between variations of parameters and the I_2 correction.

[17] In this way, the data corresponding to 6 consecutive days under solar maximum conditions, from day of year (DOY) 65 to DOY 70 of year 2001, have been gathered from the four IGS receivers depicted in Figure 4. Taking the IGS receiver JAMA (77W18N) as the reference and using GIPSY/OASIS software [see, e.g., *Zumberge et al.*, 1997], the subdaily positions of the other three receivers have been separately computed for each day. In a similar way as by *Kedar et al.* [2003] and *Fritsche et al.* [2005], this computation has been performed twice: with and without correcting the I_2 effect. Proceeding in this way, the I_2 effect on a given parameter will be obtained from the difference between both estimations.

[18] The clock of the reference receiver has been taken as the reference clock and its coordinates have been strongly constrained. Precise IGS orbits have been used, considering them fixed although their satellite clocks have been estimated. In section 4, it will be shown that the satellite clocks are the parameters that experience the biggest change due to the I_2 effect and since the orbit corrections slightly change regionally, most part of the orbit corrections can be adjusted with the estimation of the satellite clocks as well. Finally, the tropospheric delays have been slightly constrained to the values previously computed using a PPP strategy. This procedure diminishes the correlations between satellite clocks and tropospheric parameters in the regional network, providing similar results to those of the PPP strategy, but not requiring precise GPS clocks.

[19] Then, for a receiver i and a transmitter j, the model to adjust the I_2 effect in L_c and P_c (see equations (2) and (3)) by means of a zero-differenced software such as GIPSY, will be

$$(I_2)_i^j = -\frac{\boldsymbol{\rho}_i^j}{\rho_i^j}\Delta\mathbf{R}_i + c\left(T_i - t^j\right) + (T_w)_i^j + (b_c)_i^j \tag{10}$$

$$-2(I_2)_i^j = -\frac{\boldsymbol{\rho}_i^j}{\rho_i^j}\Delta\mathbf{R}_i + c\left(T_i - t^j\right) + (T_w)_i^j \tag{11}$$

where $\boldsymbol{\rho}_i^j$ is the receiver-transmitter vector, $\Delta\mathbf{R}$ is the position shift of the receiver, T_i is the receiver clock bias, t^j is the transmitter clock bias, and $(T_w)_i^j$ is the slant tropospheric delay which, in general, can be neglected because of its small value (always submillimetric).

[20] Notice that a slight mismodeling is introduced if the I_2 effect is not considered in equations (10) and (11). After merging both equations, it is clear that the effect of I_2 on the estimation of the carrier phase ambiguities will approximately be, by averaging

$$(b_c)_i^j \simeq 3\langle (I_2)_i^j \rangle \tag{12}$$

where the angle brackets represent the average value for a continuous carrier phase arc of data of a given transmitter-receiver pair as mentioned before. This relationship is confirmed in Figure 5 (blue crosses).

[21] Also, from equation (10), if applied to the reference receiver ($\Delta\mathbf{R}_i = \mathbf{0}$ and $T_i = 0$), another relationship for the I_2 effect on the satellite clock biases can be obtained:

$$ct^j \simeq 3\langle (I_2)_{\mathrm{ref}}^j \rangle - (I_2)_{\mathrm{ref}}^j \tag{13}$$

where the tropospheric term has been neglected. In Figure 5 the relationship (13) is depicted (red crosses) confirming this assumption.

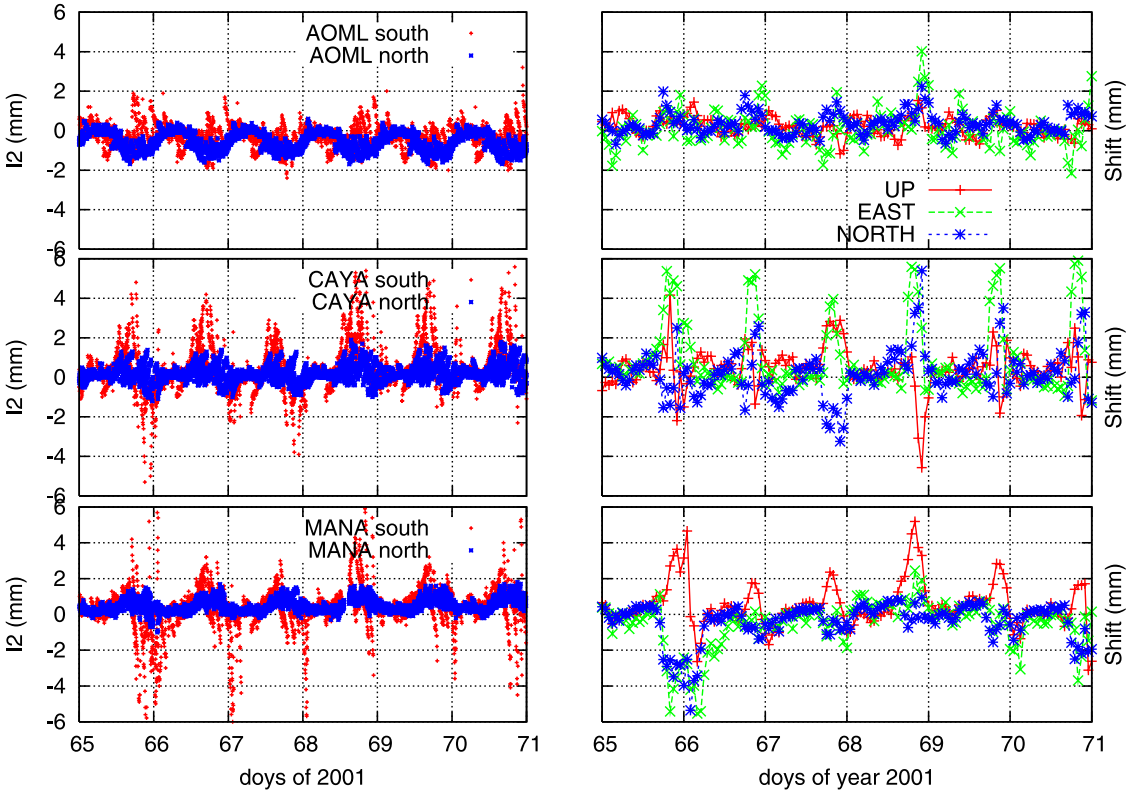

Figure 6. (left) Differential I_2 effect and (right) coordinate deviations for receivers AOML, CAYA, and MANA when JAMA is considered as the reference. In the differential I_2 effect, the northward observations are separated from the southward ones.

[22] At this point, and from equations (10), (11), (12), and (13), the next expression can be derived:

$$-\frac{\rho}{\rho}\Delta\mathbf{R}_i + cT_i \simeq (I_2)_i^j - (I_2)_{\text{ref}}^j - 3\langle (I_2)_i^j - (I_2)_{\text{ref}}^j \rangle \qquad (14)$$

It can be stated that for a nonreference receiver only the differential part of the I_2 effect contributes to the parameters deviations, as expected. The relationships contained in equations (12) and (13), represented in Figure 5, are consistent with the processed results. As it can be seen, the major part of the I_2 effect fits the deviations of the satellite clocks and the ambiguities, while coordinates and receiver clocks are only affected by the differential I_2 effect. See, for instance, Figure 5, where the north component of the receiver AOML (80W26N) deviation is represented. It can be seen that it does not vary with the absolute value of I_2.

[23] In order to understand the relationship between the differential I_2 correction and the receiver deviations in both position and clock bias, such values are depicted in Figure 6 for the three nonreference receivers. In it, the position values have been averaged using a 1-hour slide window in order to reduce the complexity of Figure 6. It is noticeable that the deviation values in position reach up to several millimeters, i.e., 1 order of magnitude greater than the typical values of daily estimations (see section 4). This is due to relative variations of the ionosphere, which are bigger in a subdaily estimation than in a daily estimations. The magnitude of these shifts in position are only related with the magnitude of the differential I_2 values (but not with the nondifferential I_2 values as was pointed out in previous works): the larger the values of the differential I_2, the bigger deviations in the position. In contrast with the results reported by *Kedar et al.* [2003] and *Fritsche et al.* [2005], where only southward displacements were reported, these shifts also seem to be dependent to the relative position of the receiver with respect to the reference but not to the absolute position of the receivers, as obtained in those previous works. Indeed, looking at Figure 6, horizontal displacements are also important for the east component of the receiver CAYA (100W17N) and there is a southward shift for MANA but northward for AOML.

[24] In the differential I_2 corrections depicted in Figure 6, the northward observations are distinguished from the southward observations. At these latitudes, most of the observations are northward and therefore a negative differential I_2 correction will imply a reduction in the northward ranges following equation (14) and, as a consequence, a northward shift of the receiver position. This is the case for receivers AOML and CAYA, where the differential I_2 values are negative at the local noon (positive for MANA) for the northward observations. This is translated into a northward deviation for AOML (southward for MANA) in the position domain. A enlarged view of Figure 6 has been plotted for AOML in Figure 7 in order to see the correlation between both values more clearly.

[25] As a final comment, it can be advanced that in spite of using an incomplete model to adjust the I_2 correction in the differential estimation (without considering the effect on orbits), some of the obtained results with this method will

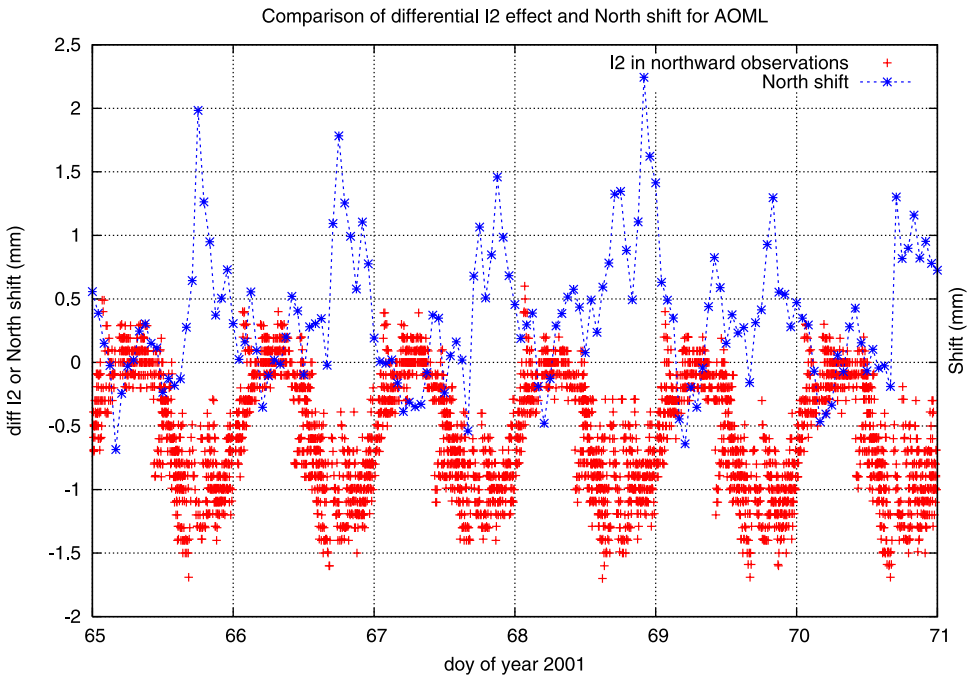

Figure 7. Relationship between the AOML north shift and the differential I_2 effect for northward observations.

be similar to those using a complete model in a global estimation. In fact, one way to proceed with a global computation is to constrain the coordinates of a subset of receivers (fiducial receivers) and to apply a similar strategy to the differential one but estimating orbits as well. In this way, it shall be expected that the major part of the I_2 effect will be adjusted by clocks and orbits in a global estimation, and the receiver parameters (position and troposphere) will be mainly related to the relative values of the I_2 correction among receivers.

4. Effect of the I_2 Correction on Global Estimations

[26] For the global estimation, the followed strategy is different from the one applied for differential positioning (section 3) or the one used by *Kedar et al.* [2003] or *Fritsche et al.* [2005]. All those strategies were based on two computations: correcting and not correcting the I_2 effect from the observables. In this way, the deviations that the I_2 effect produces on the parameter estimations are obtained from the difference between both computations.

[27] In this section, the global estimations have been derived from pseudomeasurements built from a geodetic model (in this case, provided by GIPSY) plus the corresponding I_2 effect for the current observation. In this way, the prefit residuals (i.e., the Kalman filter inputs) correspond to the I2 contribution only. Any other mismodeling is not present in the filter input, so it will not produce any deviation in the estimated values. Thus the I2 impact on geodetic estimations is obtained in a straightforward way.

[28] Although a nonfiducial approach has been followed, a precise computation of the receiver positions is not required with this strategy in order to obtain the references for a seven-parameter Helmert transformation. Notice that from section 3, the distribution of receivers is a key point in the I_2 effect on the geodetic estimations. Indeed, if most of the receivers were located in the Northern Hemisphere, the I_2 effect on their positions would be small. This has been taken into account by selecting a worldwide distribution of receivers as close as possible to a uniform one.

[29] After the estimation of the parameter deviations with the GIPSY/OASIS software and the application of the Helmert transformation, a simple recovery model is used that allows to relate the I_2 effect with the deviations of the parameters. This model can be written as

$$(I_2)_i^j = -\frac{\boldsymbol{\rho}_i^j}{\rho_i^j}\Delta\mathbf{R}_i + (T_w)_i^j + \frac{\boldsymbol{\rho}_i^j}{\rho_i^j}\Delta\mathbf{r}^j - ct^j + cT_i + (b_c)_i^j \quad (15)$$

where $\Delta\mathbf{r}^j$ is the shift vector for the satellite j, and the rest of the parameters are the same as those considered in equation (10), except for the tropospheric delay $(T_w)_i^j$ which now also includes a model for the tropospheric gradients.

[30] The first two terms in the right member of equation (15) correspond to the projection on the LOS of the receiver-dependent parameters (position and troposphere). The third term corresponds to the LOS projection of the orbit error, and the last three terms correspond to bias parameters (clocks and ambiguities). In section 3, it was shown that the receiver-dependent parameters were only affected by the differential part of I_2, regarding to the reference receiver. In Figure 8, the receiver-dependent parameters affected by the I2 effect are separately represented according to the satellite orbits and the bias parameters. This is performed during 36 days of year 2003 (once

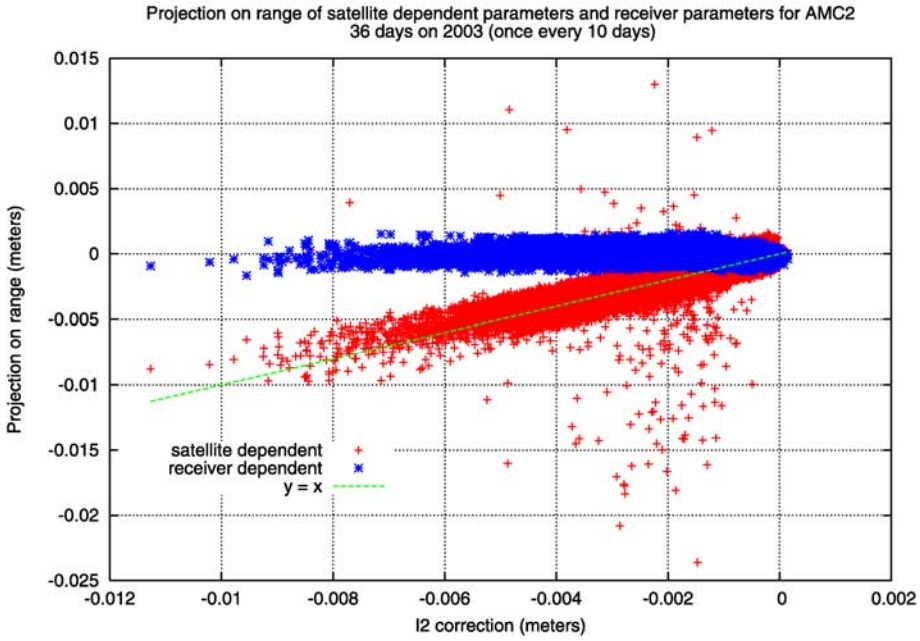

Figure 8. Relationships between the I_2 correction for IGS receiver AMC2 (105W39N) and the satellite-dependent parameters (crosses), and the receiver-dependent parameters (asterisks), projected on range in both cases. The 69,000 observations are represented corresponding to 36 days of year 2003 (once every 10 days). Observations below 15° are not depicted. The line shows that the I_2 effect is basically adjusted to the satellite-dependent parameters.

every 10 days) for the IGS receiver AMC2 (105W39N, reference clock receiver). From Figure 8, it is confirmed that the satellite orbits and the bias are the most affected parameters by the I_2 correction while the receiver-dependent ones (tropospheric and position estimations) only represent a small part of the I_2 correction.

[31] Figure 8 corresponds to IGS station AMC2 (which clock is taken as reference). For other receivers the I_2 effect on their clock biases can reach up to few millimeters due to the correlation with the other bias parameters (satellite clocks and ambiguities).

[32] In Figure 9, the relationship in equation (12), which was obtained for differential positioning, is confirmed and is still valid for global estimations, on an average way. In this way, deviations of the carrier phase bias estimations have negative values for Southern Hemisphere receivers and positive values for Northern Hemisphere receivers.

4.1. Effect on Satellite Clocks and Positions

[33] The results in Figure 8 show that when a complete modeling of the I2 effect is performed, it mostly affects the satellite orbit and bias dependences rather than the receiver parameters.

[34] In order to understand such dependences, we have to take into account that in a global geodetic estimation, a set of reference coordinates, which are considered fixed, is needed. In a fiducial strategy, this can be done for a subset of receivers and, in a nonfiducial strategy, for all the network (on an average way after a Helmert transformation). In Figure 10, a scheme of the I_2 effect on the satellite positions is represented for three satellites located in a dayside meridian (i.e., when the I_2 effect is larger). Figure 10 is similar to Figure 1 of *Kedar et al.* [2003] but considering receiver positions fixed instead of the satellite ones.

[35] Following Figure 10, the largest range variations will occur for the observation corresponding to the lowest latitude receiver: northward observations will increase their range (represented by plus in Figure 10), while southward observations will decrease it (minus in Figure 10). In Figure 10 the I_2 uncorrected satellite position (origin of bold arrows) is determined by the range uncorrected measurements (solid lines) from ground receivers. In this way, when the I_2 effect is taken into account, range variations will occur up to the dashed circle arcs, being the I_2 satellite corrected positions (head of bold arrows) determined by the intersection of the dashed arcs.

[36] The resulting effect is a systematic northward shift of the satellite position, being this displacement larger when the satellite is at higher latitude. However, in a PPP strategy as that followed by *Kedar et al.* [2003], in which the satellite positions are considered fixed, the positions of receivers will be deviate southward.

[37] The situation described in the preceding paragraph will mainly occur for dayside observations. For nightside observations, the shift in satellite positions will be negligible. Since all the satellite positions are connected by the dynamical model, the orbital parameters will be adjusted to take into account such nonuniform variations. In this way, the resulting orbit will present a northward displacement for

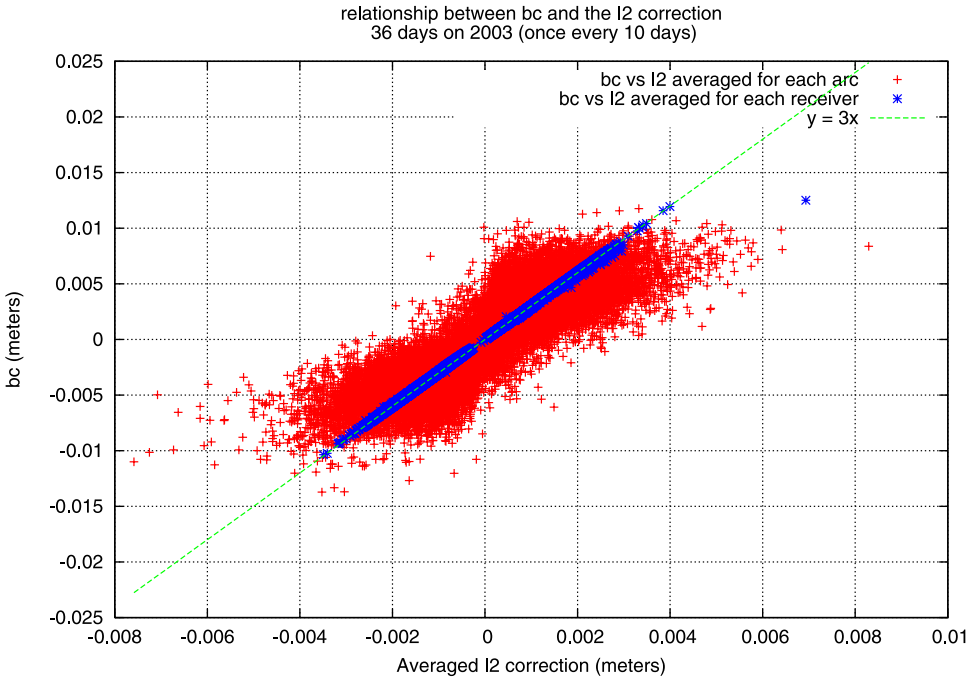

Figure 9. Relationship between the estimated carrier phase biases (b_c) and the I_2 effect, for each individual arc and the daily average for each receiver. The agreement on the straight line shows that this relationship is basically the same as equation (12).

dayside observations, when the satellite is at high latitudes, and a southward shift when the satellite is, for instance, at low latitudes or nightside observations. A confirmation of this is depicted in Figure 11, where the northward shift of the satellite positions are represented according to the satellite latitude and separating day and nighttime data, from DOY 103 of year 2003. From Figure 11, it can be seen that the mean effect consists on a negative displacement of the z component (i.e., latitudinal component at low latitudes) of the overall orbit, justifying the behavior reported by previous works.

[38] This negative shift along the Z axis shown in Figure 11 is a common feature for all the analyzed days. In Figure 12, the three components of the mean displacement vector are represented for each day and for each satellite. In it, these daily mean displacements are at the millimeter level for X and Y components. Regarding the Z component, it achieves larger values than the other two, being these displacements correlated with the ionization degree of the Ionosphere. This correlation is clearer if the averaged value is represented for all the satellites (Figure 12, top), then the resulting averaged Z shift is similar to the Z component of the geocenter given by *Fritsche et al.* [2005]. In order to see this correlation, the global electron content (GEC) value is represented for the same days in Figure 12 (top). The GEC is defined by *Afraimovich et al.* [2006] as the total number of free electrons of a GIM that can be measured in GECUs (1 GECU = 10^{32} electrons) and computed from a GIM as

$$\mathrm{GEC} = \sum_i T_i S_i \qquad (16)$$

where the sum is extended to all the grid points of the GIM, being T_i the total electron count (TEC) value at the IPP and S_i the corresponding area.

[39] Among this daily mean displacement of the orbits, there is still a subdaily shift of several millimeters that depends on the local time. In Figure 13, the residual part of the orbit displacements (i.e., after subtracting the daily mean value of Figure 12) is represented according to the local time and latitudes of the satellites. As expected (see Figure 11), there is still a northward displacement of several millimeters at day time, positive for high latitudes and negative for low latitudes. The radial component has also a subdaily trend of few millimeters that depends on both the latitude and the local time: this is related to the range shortening in the Northern Hemisphere observations (a range enlargement in the Southern Hemisphere ones). The subdaily shifts contained in Figure 13 correspond to average values for the year 2003, and the dispersion of these values is represented by means of their standard deviation in the right panels. These dispersion values are also highly correlated with the ionization degree of the ionosphere.

[40] In conclusion, taking into account the daily mean and subdaily residuals, the I_2 term effect on orbits can reach up to 1 cm, i.e., comparable with the final IGS orbit accuracies.

[41] Finally, the 2003 mean values of the satellite clock shifts caused by the I_2 effect are represented in the bottom panels. These values are several times greater than the ones of the orbit, being the most important parameter deviation of the I_2 effect. Unlike in differential positioning (see section 3), the I_2 effect on satellite clocks does not follow now the relationship in equation (13). The reason of this different dependence can be explained when equation (15)

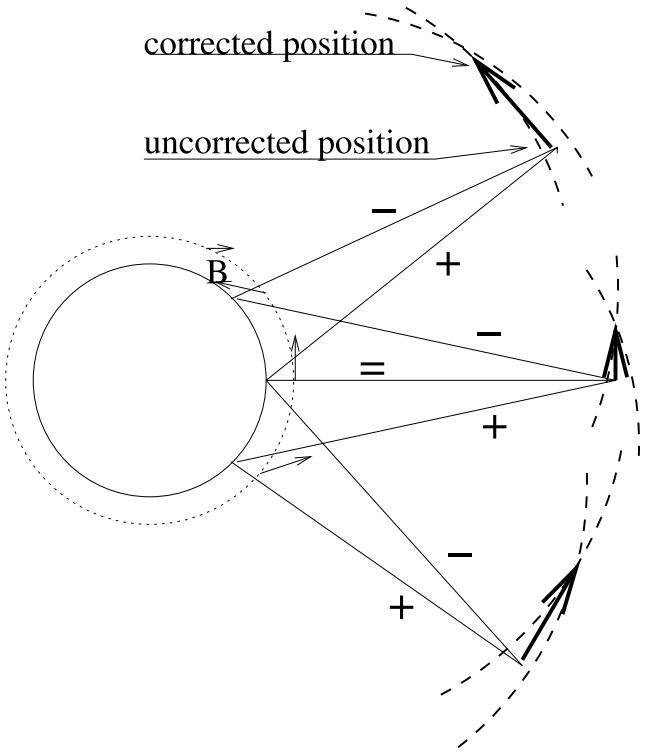

Figure 10. Schematic representation of the I_2 effect on satellite positions for three different satellites located along a dayside meridian as they are tracked from three ground receivers. The relative direction between the magnetic field **B** (represented over the dashed circle at the ionospheric height) and the line of sight determine the range increasing (represented as plus) or decreasing (minus). These range variations produce a shift in satellite positions represented by the wide arrows: the uncorrected satellite position, arrow's origin, is the intersection of two circles determined from the uncorrected range observations taken in two different receivers; see dotted lines. The corrected position (arrow heads) can be geometrically deduced in a similar manner but with the corrected ranges; see signs and dashed circles. It can be seen that the main effect is a northward displacement (greater on high latitudes) of the satellite positions.

is averaged over all the observations with a common satellite. Then, after neglecting the receiver-dependent terms, the remaining expression is

$$\frac{1}{N_{\text{sta}}}\sum_i (I_2)_i^j = \frac{1}{N_{\text{sta}}}\sum_i (b_c)_i^j + \frac{1}{N_{\text{sta}}}\left(\sum_i \frac{\boldsymbol{\rho}_i^j}{\rho_i^j}\right)\Delta\mathbf{r}^j - ct^j \quad (17)$$

where the sum extends over all the stations (N_{sta}) that have data from satellite j at this epoch.

[42] In a differential or regional solution, all the involved stations would have a similar I_2 effect. Thus, if the second term in the right hand member of equation (17) was interpreted as part of the satellite clock (as already done in section 3), similar relationships to those in the regional study (section 3) can be obtained.

[43] However, in a global estimation, the values of the I_2 effect are very different from one receiver to another, so the left hand member of equation (17) will have, in general, small values. In this way, the satellite clock correction would be related with the rest of satellite-dependent parameters by

$$ct^j \simeq \frac{1}{N_{\text{sta}}}\sum_i (b_c)_i^j + \frac{1}{N_{\text{sta}}}\left(\sum_i \frac{\boldsymbol{\rho}_i^j}{\rho_i^j}\right)\Delta\mathbf{r}^j \quad (18)$$

In Figure 14, the relationship between the two members of equation (18) is displayed for the data corresponding to DOY 103 of year 2003. This linear relationship has a correlation coefficient of 0.96 (0.94 for all the year 2003).

[44] Summarizing, the I_2 effect on satellite clocks is typically the greatest one: it can be larger than 1 centimeter, i.e., comparable with the reported IGS clock estimations accuracy (http://igscb.jpl.nasa.gov/components/prods.html). Hence the results of applying a realistic I_2 corrections should be of high interest for the timing community, in particular, in order to provide even more accurate clocks.

4.2. Effect on Receiver Positions

[45] Regarding the shifts in receiver positions, the results confirm those obtained in section 4.1. Indeed, the shifts depend on the relative values of the I_2 effect (with respect to the neighbor receivers), rather than on the values themselves. This is because of the Helmert transformation adjust the final receiver positions to its reference values. In this sense, those receivers with larger values of I_2 will present a southward displacement, while those with smaller values of I_2 will present a northward displacement. This can be seen in Figures 15 and 16, where a clear southward displacement (generally smaller than 1 mm) is shown only for the receivers close to the geomagnetic equator. Moreover, high-latitude receivers present northward displacements.

[46] These results are not in agreement with those of *Kedar et al.* [2003] where all the displacements are mainly southward and of about several millimeters. The reason for such disagreement is that is the study by Kedar et al., the I_2 effect is only adjusted with the receiver parameters, as mentioned in section 1.

[47] On the one hand, the current results do not fully agree with the conclusions of *Steigenberger et al.* [2006] or *Fritsche et al.* [2005] because no northward displacement was reported for high-latitude receivers, although some of this can be appreciated in their figures for the Antarctic receivers. This is probably due to the way STEC was computed, obtaining smoothed values of it, as shown in the example of Figure 1. On the other hand, there is a clear difference when considering the receivers close to the SAA (see Figure 2): In the papers by *Kedar et al.* [2003] and *Fritsche et al.* [2005], because of the simpler magnetic dipolar model employed, there is also a southward displacement for these low-latitude receivers that does not appear in the presented results, where a more realistic geomagnetic model is used. Moreover there is another important difference: the spatial distribution of the Fritsche et al. set of receivers (a subset of IGb00 net) contains many more receivers in the Northern Hemisphere, mainly at mid-high

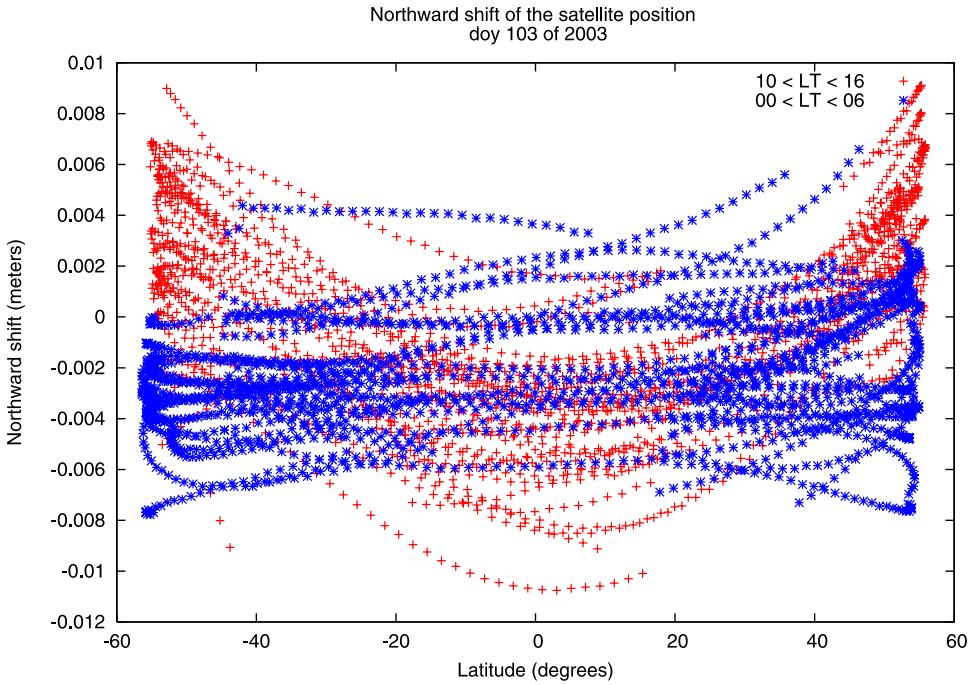

Figure 11. Representative example of the I_2 effect in the north component shift in the satellite position. The data correspond to DOY 103 of year 2003. It can be seen that all the satellites basically experiment a southward shift, except for those in high latitudes at day time.

latitudes (50% of receivers with latitudes greater than +30 degrees). Then, when the Helmert transformation is done, these northern receivers have an overweight in the transformation, diminishing the apparent displacements of its coordinates. In our case we selected a more homogeneous distribution of receivers (only 35% of receivers with latitudes greater than +30 degrees), in such a way that northward and southward displacements are obtained, due to the more evenly weighted scheme in the corresponding Helmert transformation.

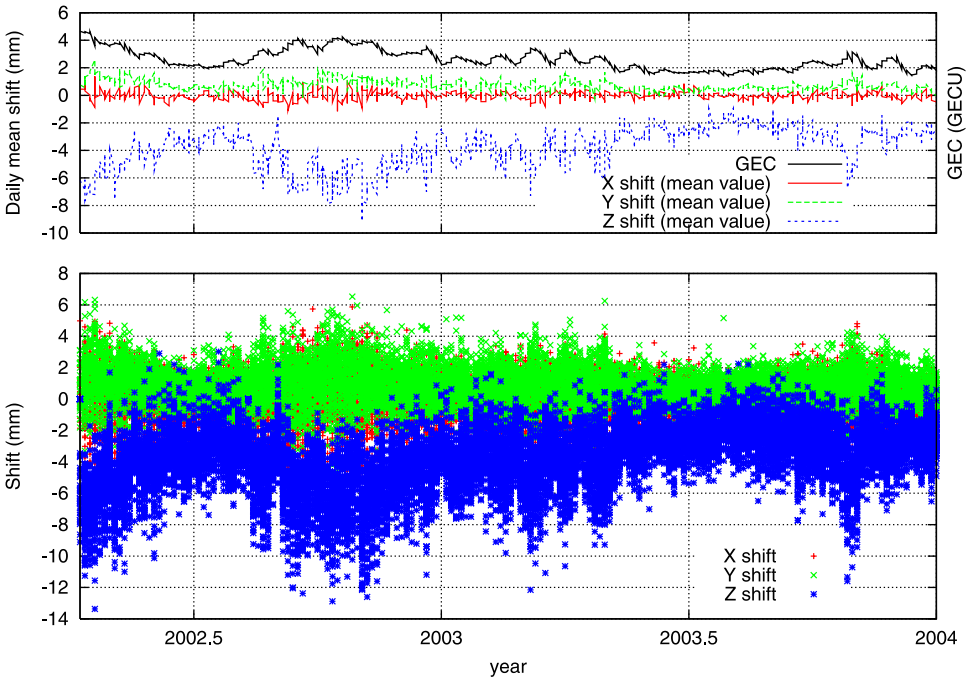

Figure 12. (bottom) Components of the daily averaged shift vector for every satellite. (top) Daily mean for all the satellites for each component. In order to see the relationship with the ionospheric activity, the mean daily GEC value is also depicted.

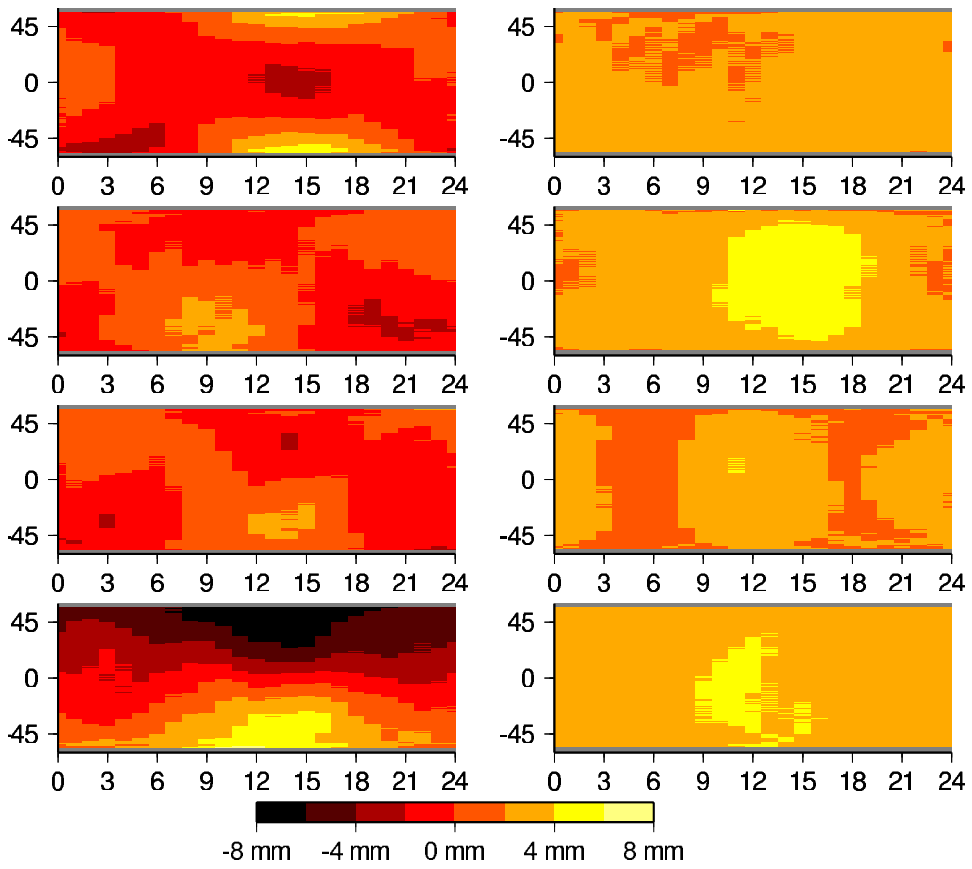

Figure 13. Residual effect on orbit parameters (from top to bottom, north, east, radial, and clock). (left) Averaged value over 2003 and (right) corresponding standard deviations.

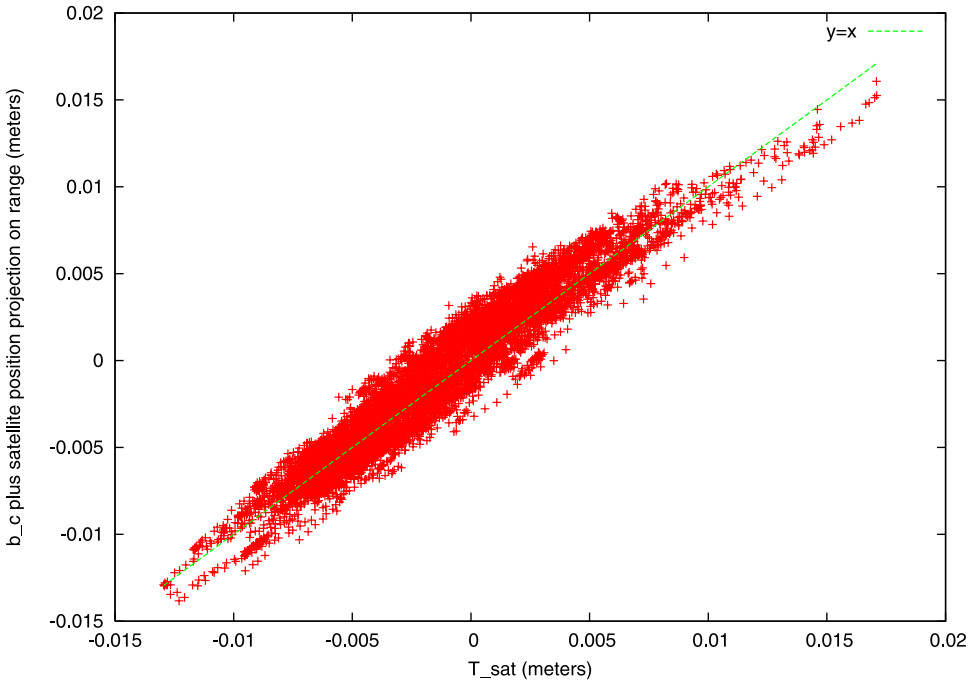

Figure 14. Relationship between the two members of equation (18) for DOY 103 of year 2003.

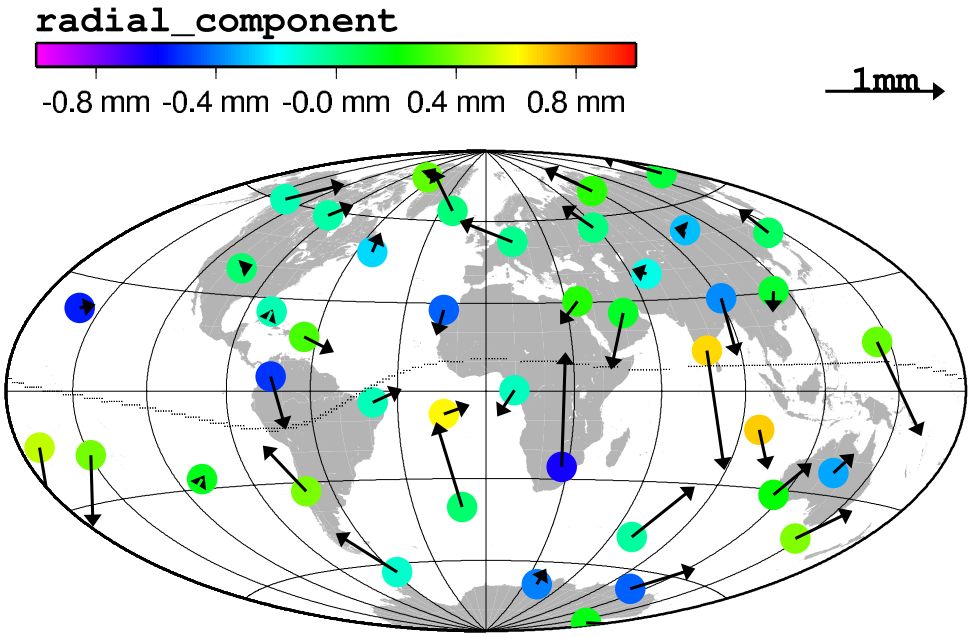

Figure 15. Mean I_2 effect on receiver positions for 21 months of GPS observations (from DOY 100 of year 2002 up to DOY 365 of year 2003). Only receivers with more than 200 days of data are represented.

[48] The results shown in Figures 15 and 16 correspond to the mean values of the shift vectors from year 2003 and the last 9 months of year 2002, but these shifts are not constant over time. An idea of the dispersion of these values can be derived from Figure 17, where all the components of the shift vectors are related to the coordinates of the receivers. In Figure 17, receivers close to the SAA are excluded because their anomalous I_2 effect. Although the shift of the coordinates can reach up to more than one millimeter, the corresponding effect on coordinates repeatabilities is smaller: it has to be taken into account that the coordinates repeatability is only directly affected by the dispersion of these daily shifts. Notice that these dispersions are very small: in general, for a given receiver, it reaches up

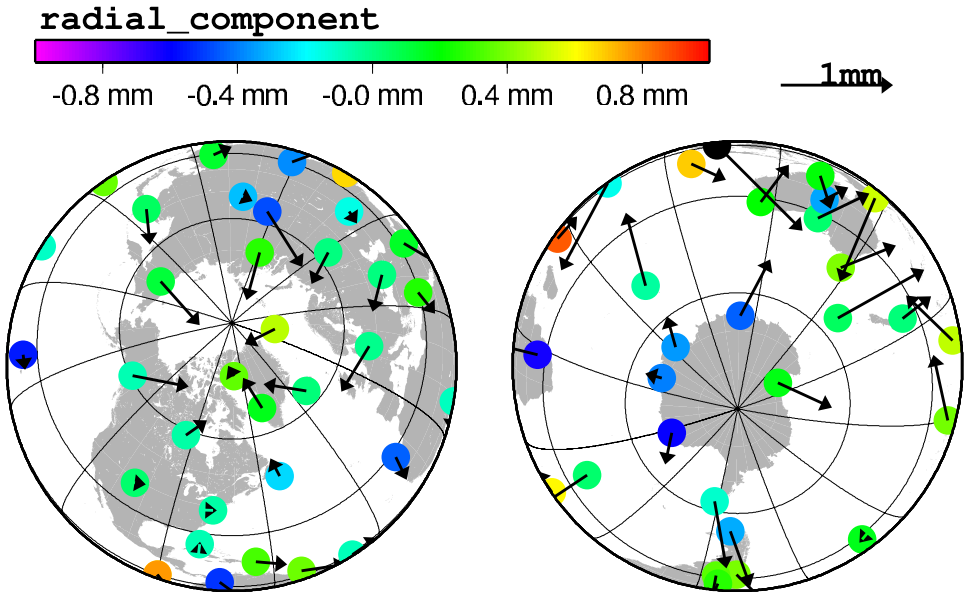

Figure 16. Same as in Figure 15 but using polar projections. In this case, receivers with at least 100 days of data are plotted. The northward shift of the high-latitude receivers is confirmed.

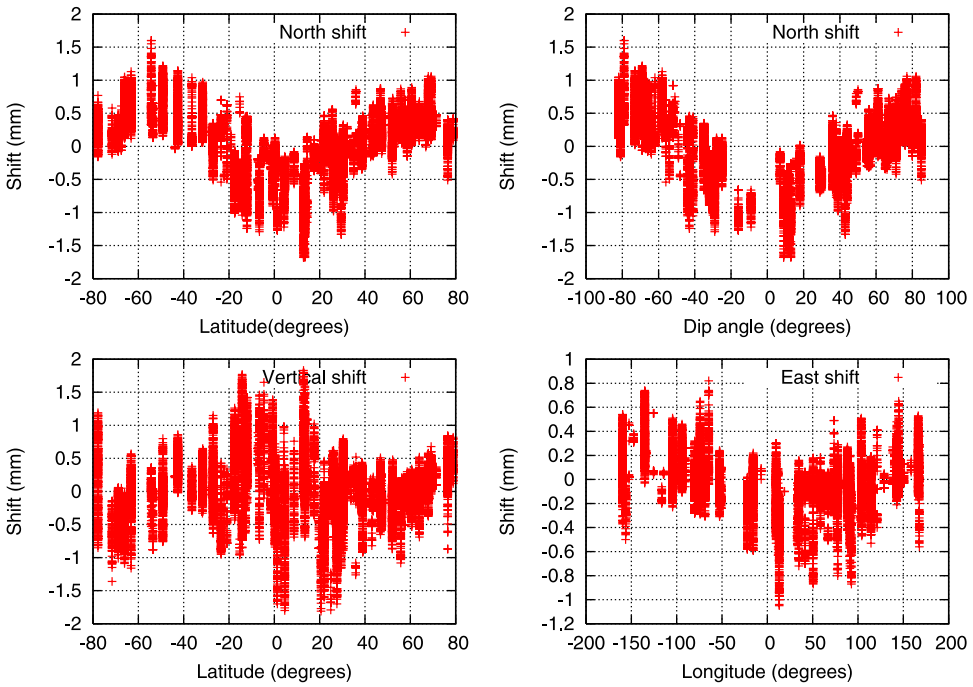

Figure 17. Daily shifts for all receivers (excluding those close to the SAA). North shift (top left) as a function of the geographical latitude and (top right) as function of the dip angle. (bottom left) Vertical shift as a function of the geographical latitude. (bottom right) East shift as a function of the longitude. These shifts are, in general, smaller than 1 mm with a standard deviation of few tenths of mm. The data sets correspond to the period from April 2002 to December 2003.

to just a few tenths of millimeters. This implies that a small, if any, improvement can be expected in the coordinates repeatability after applying I2 correction.

[49] Regarding the vertical components, there is not a clear systematism on their values. However, it seems that the major effects on this component occur in case of low-latitude receivers (where the I_2 gradients are greater), while for high-latitude receivers this vertical shift is small (positive for northern receivers and negative for southern receivers).

[50] The east component of the shift vector is represented versus the longitude (instead of the latitude) in Figure 17 since there is a slight dependence between both magnitudes: The I_2 effect on low-longitude receivers consists of a westward displacement and eastward for high-longitude receivers. This is probably related with the local minimum that the magnitude of the magnetic field has at low longitudes.

[51] Finally, the north shift appears to be linked to the dip angle (Φ_B) of the local magnetic field (i.e., the angle between the magnetic field vector and the local horizon with inverted sign). In this way negative displacements occur for low Φ_B and positive displacements for high values of Φ_B.

[52] In Figure 18, the variation along the year 2003 of this shift vector is represented for 5 representative receivers: WHIT (61N135W), YSSK (47N143E), KOKB (22N160W), GUAM (13N145E), CAS1 (66S111E). Because of the noise of several components of the shift vector, a running mean along 10 days has been used in order to reduce it. Regarding Figure 18, the relationship between the magnitude of the shift vector components and the ionization degree (see the GEC on Figure 12, top) is clearly shown. It is also noticeable that the largest horizontal displacements occur for the highest latitude receivers (with a well-defined northward direction) and for the lowest latitude receivers (with a well-defined southward direction). However, the middle-latitude receivers show smaller horizontal shifts in a direction that it is not so well defined as in the other three receivers.

[53] From the results represented in Figures 17 and 18, a simple lineal model can be adjusted for the latitudinal shift (Δn) on the receiver positions:

$$\Delta n = m\mathrm{GEC}\cos(2\Phi_B) + b \tag{19}$$

This expression is suitable to explain performances, such as the one of receiver KOKB in Figure 18 (around day 230, 2003), that presents a local dip angle of about 37°. So the expected shift is very small, without a well-defined azimuth.

[54] In Figure 19, the implementation of this linear model is represented. As it can be seen, there is a different performance for low- and high-latitude receivers, because the GEC is basically determined with the low-latitude grid points of a GIM. The values for the adjusting coefficients are also written in Table 1, where the prediction capabilities of this model are shown in the last column through the reduction of the RMS of the north component of the shift vector.

5. Summary and Conclusions

[55] The aim of this paper has been to contribute to a better understanding of the I_2 term effect on geodetic

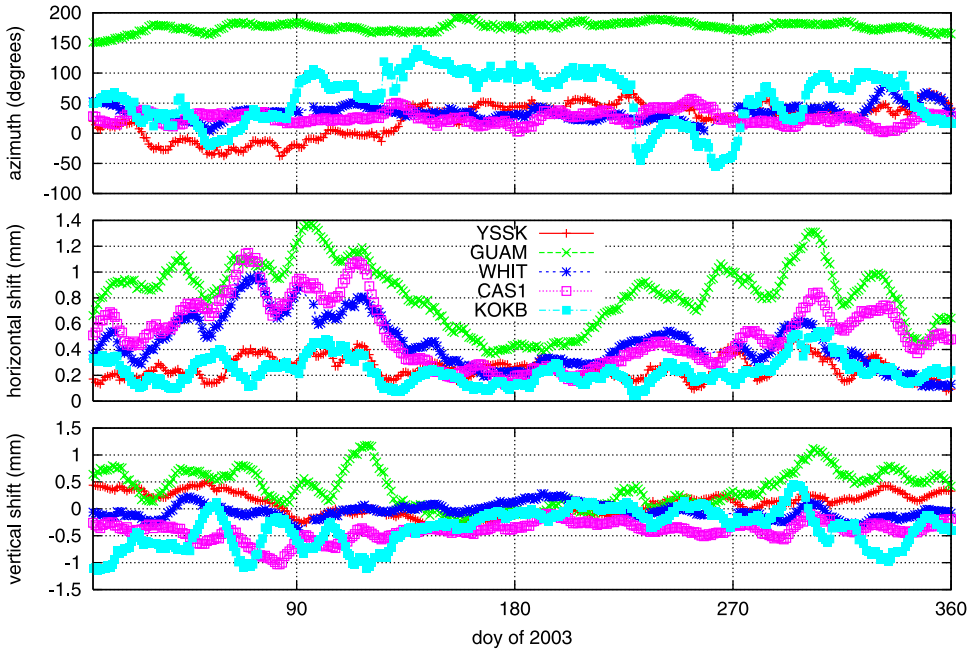

Figure 18. Daily components of the shift vector for five receivers: WHIT (61N135W), YSSK (47N143E), KOKB (22N160W), GUAM (13N145E), CAS1 (66S111E). (top) Azimuth. (middle) Horizontal shift. (bottom) Vertical shift. A running mean for 10 days using a slide window has been applied in order to reduce the noise. Notice the clear southward and northward displacements experienced by low- and high-latitude receivers, respectively.

estimates. In this way, a set of relationships between this effect and its impact over the parameter deviations have been presented and discussed in a quantitative and qualitative way.

[56] A new and easy way of computing the I_2 effect has been presented, that differs in two aspects with respect to previous works. First, the STEC is computed using the geometry-free pseudorange instead of using the TEC values from a GIM, or any GIM software in general. Also, second, an accurate model has been used to calculate the geomagnetic field. In this way, improvements up to 60% can be

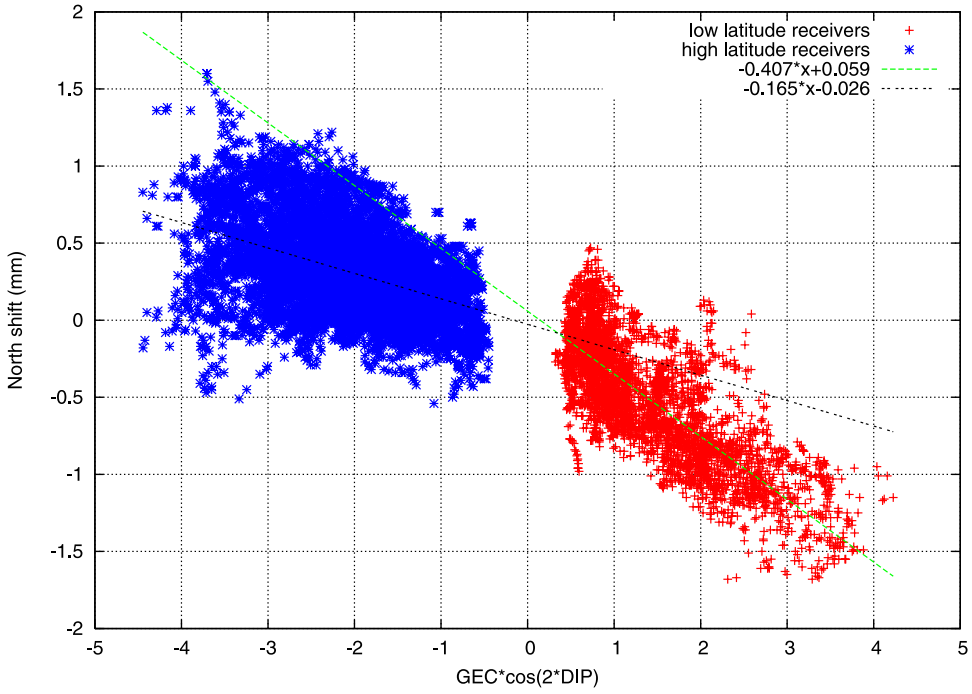

Figure 19. Latitudinal shift for all the studied period of all the receivers (excluding those close to the SAA) versus the model of equation (19).

Table 1. Parameters for the Linear Model of Equation (19)

	m, mm/GECU	b, mm	Reduction on RMS,[a] %
Low-latitude receivers	−0.407	0.059	62
High-latitude receivers	−0.165	0.026	40

[a]Prediction degree of this model for the actual latitudinal shift.

achieved in the I_2 term computation. Such improvements are directly translated into the geodetic estimations.

[57] Using differential positioning techniques, it has been shown that the deviations of the receiver positions are driven by the differential (among receivers) I_2 effect, instead of their absolute values. These deviations can reach up to several millimeters, 1 order of magnitude larger than the typical daily effect. This is due to that the subdaily variation of the I2 effect (driven for the large electron content variation in terms of local time) is greater than the day-to-day variation. However, in these regional solutions, the most affected parameters by the I_2 effect would be the satellite clocks, which variations would be adapted to this effect.

[58] In global geodetic computations, a new method has been used that allows to understand how I_2 affects the parameter estimations. Following this procedure, the conclusion of the differential positioning study was confirmed, i.e., that the I_2 effect is adjusted mainly by the satellite-dependent parameters (orbits and clocks), while the effect on the receiver-dependent parameters is clearly small because they are only affected by the differential or relative value of the I_2 effect (i.e., compared to the values of the other receivers of the network).

[59] It has also been shown that the most affected parameter is the satellite clock, which can show deviations greater than 1 cm. These deviations depend on the latitude and local time of the satellite position, achieving the largest values at local daytime, positive in the Southern Hemisphere and negative in the Northern Hemisphere. This effect is comparable with the accuracy of the Final IGS products.

[60] Satellite positions are affected by a global southward displacement of the orbits of several millimeters. The amount of this displacement is related to the ionization degree of the ionosphere, that determines the values of the I_2 effect. This result agrees with the geocenter displacement in the z component found by other authors. Among these global displacements of the orbits, there is still a subdaily part of the deviations of the satellite positions mainly in the latitudinal component. This effect can reach up to several millimeters and depends on the latitude and on the local time. The overall effect on orbits (daily and subdaily) can be also of the same order of magnitude than the final IGS orbit accuracy.

[61] The I_2 impact on receiver positions is usually smaller than 1 mm (for the period studied in this work). The most significant displacement on the receiver positions occurs, as was also noted by previous authors, in the north-south direction. However, in discordance with the results of *Kedar et al.* [2003] and *Fritsche et al.* [2005], a latitudinal dependence on the sign of this displacement has been found. Indeed, high-latitude receivers would be shifted northward while the low-latitude ones would be moved southward. This agrees with the idea that the receiver position is affected by the differential I_2 effect. In this way, receivers with large values of the I_2 effect are shifted southward, while those with small values are shifted northward. Moreover, it has been found that such latitudinal dependence is modulated by the ionization degree of the Ionosphere, providing the corresponding model.

[62] Finally, the authors of this work think that this effect should be taken into account in routinary geodetic computations because (1) the contribution of the I_2 effect is not negligible (several centimeters in range), (2) the algorithms presented in this work are easy to implement (they do not require the previous computation of a GIM or associated software), and (3) the I_2 effect on satellites clocks and orbits is significant and should be taken into account to improve its accuracy.

[63] **Acknowledgments.** We thank the IGS community for stimulating this work, and the availability of the data sets used in this paper. This work has been partially supported by the Spanish projects ESP2004-05682-C02-01 and ESP2007-62676. The authors are grateful to Angela Aragon-Angel and Alberto Garcia-Rigo for their support in improving the English of the initial manuscript.

References

Afraimovich, E. L., E. I. Astafyeva, and I. V. Zhivetiev (2006), Solar activity and global electron content, *Dokl. Earth Sci.*, *6*, 921–924, doi:10.1134/S1028334X06060195.

Bassiri, S., and G. Hajj (1993), High-order ionospheric effects on the global positioning system observables and means of modeling them, *Manuscr. Geod.*, *18*, 280–289.

Fritsche, M., R. Dietrich, C. Knöfel, A. Rülke, S. Vey, M. Rothacher, and P. Steigenberger (2005), Impact of higher-order ionospheric terms on GPS estimates, *Geophys. Res. Lett.*, *32*, L23311, doi:10.1029/2005GL024342.

Hernández-Pajares, M. (2004), Ionosphere IGS WG position paper, paper presented at the IGS Technical Meeting, Bern, Switzerland.

Kedar, S., G. A. Hajj, B. D. Wilson, and M. B. Heflin (2003), The effect of the second order GPS ionospheric correction on receiver positions, *Geophys. Res. Lett.*, *30*(16), 1829, doi:10.1029/2003GL017639.

Klobuchar, J. A. (1978), *Ionospheric Effects on Satellite Navigation and Air Traffic Control Systems*, *AGARD Lect. Ser.*, vol. 93, Advisory Group for Aerospace Res. and Dev., North Atlantic Treaty Org., Brussels.

Lanyi, G. E., and T. Roth (1988), A comparison of mapped and measured total ionospheric electron content using global positioning system and beacon satellite observations, *Radio Sci.*, *23*(4), 483–492.

Mannucci, A. J., B. D. Wilson, D. N. Yuan, C. H. Ho, U. J. Lindquister, and T. F. Runge (1998), A global mapping technique for GPS-derived ionospheric total electron content measurements, *Radio Sci.*, *33*, 565–582.

Steigenberger, P., M. Rothacher, R. Dietrich, M. Fritsche, A. Rülke, and S. Vey (2006), Reprocessing of a global GPS network, *J. Geophys. Res.*, *111*, B05402, doi:10.1029/2005JB003747.

Tsyganenko, N. A. (2003), A set of FORTRAN subroutines for computations of the geomagnetic field in the Earth's magnetosphere (Geopack), Univ. Space Res. Assoc., Columbia, Md.

Zumberge, J. F., M. B. Heflin, D. C. Jefferson, M. M. Watkins, and F. H. Webb (1997), Precise point positioning for the efficient and robust analysis of GPS data from large networks, *J. Geophys. Res.*, *102*, 5005–5017.

M. Hernández-Pajares, J. M. Juan, and J. Sanz, Research Group of Astronomy and Geomatics, Technical University of Catalonia (gAGE/UPC), Mod. C3, Campus Nord UPC, Jordi Girona 1, E-08034 Barcelona, Spain. (manuel@mat.upc.es)

R. Orús, ESA/ESTEC/TEC-EEP, Keplerlaan 1, NL-2201 AZ Noordwijk ZH, Netherlands.